Polymer 50 (2009) 418–427

Contents lists available at ScienceDirect

Polymer

journal homepage: www.elsevier.com/locate/polymer

Amphiphilic block copolymers bearing strong push–pull azo chromophores: Synthesis, micelle formation and photoinduced shape deformation

Dongrui Wang, Junpeng Liu, Gang Ye, Xiaogong Wang*

Department of Chemical Engineering, Laboratory for Advanced Materials, Tsinghua University, Beijing 100084, PR China

ARTICLE INFO

Article history:
Received 31 August 2008
Received in revised form
9 November 2008
Accepted 13 November 2008
Available online 19 November 2008

Keywords:
Atom transfer radical polymerization
Azobenzene-containing block copolymers
Amphiphilic

ABSTRACT

In this work, a series of amphiphilic diblock copolymers bearing strong push–pull type azo chromophores was synthesized through post-polymerization azo-coupling reaction scheme. The copolymers (P(CNAZO$_m$-*b*-MAA$_n$)), composed of 2-(*N*-ethyl-*N*-(4-(4′-cyanophenylazo)-phenyl)amino)ethyl methacrylate (CNAZO) and methacrylic acid (MAA) blocks, were obtained through four-step reactions. Firstly, precursor diblock copolymers (P(EMA$_m$-*b*-*t*BMA$_n$)) were obtained through sequential two-stage ATRP reactions of 2-(*N*-ethyl-*N*-phenylamino)ethyl methacrylate (EMA) and *tert*-butyl methacrylate (*t*BMA). Then, 4-amino-4′-cyanoazobenzene chromophores were introduced by azo-coupling reaction of P(EMA$_m$-*b*-*t*BMA$_n$) with diazonium salt of 4-aminobenzonitrile. Finally, P(CNAZO$_m$-*b*-MAA$_n$) was obtained through selective hydrolysis of the *tert*-butyl ester linkages in the *t*BMA blocks. Three block copolymers with the same CNAZO block length ($m = 100$) and different MAA block lengths ($n = 5, 13, 23$) were prepared by this method. The polymer and copolymers prepared in the process were characterized by GPC, ^{1}H NMR, UV–vis, DSC and TGA measurements. Results show that P(CNAZO$_m$-*b*-MAA$_n$) forms spherical micellar aggregates by gradually increasing the water content in THF/H_2O mixtures. The diameters of the spherical aggregates are related to the composition of the block copolymers and the water-adding rate. The block copolymer with larger molecular weight of the hydrophilic MAA block forms the aggregates with the smaller average size. The increase of the water-adding rate also shows an effect to reduce the diameters. Upon irradiation with a linearly polarized Ar^+ laser beam, the spherical aggregates can be elongated in the light polarization direction. The deformation degree shows an almost linear dependence on the light irradiation time in the testing period. The deformed aggregates can recover the original spherical shape after thermal annealing at a temperature above T_g of the block copolymer.

1. Introduction

Amphiphilic block copolymers, consisting of covalently linked hydrophobic block and hydrophilic block, have attracted considerable attention in recent years because of their unique chain architecture and interesting properties [1–9]. Induced by selective solvents, amphiphilic block copolymers can self-assemble into a variety of well-defined supramolecular structures such as spheres, vesicles, rods and lamellae [7–9]. In one of the simplest cases, amphiphilic block copolymers can form uniform micellar spheres with a hydrophobic core and a hydrophilic corona in aqueous media [4,5]. In organic solvents, amphiphilic block copolymers can form reverse micelles with a hydrophilic core and hydrophobic corona. Depending on the relative size of the core and corona, the micellar aggregates have been named as ‘star-like’ and ‘crew-cut’ micelles [7,10–13]. In general, uniform micelles can only be obtained from block copolymers with narrow dispersity in both the molecular weight and the block length [14,15]. Other more sophisticated structures, such as vesicles, hollow tubes, can be obtained by adjusting polymer structure and preparation conditions [7,8,16,17]. In all the cases, the polymer structure and relative size of the hydrophobic block to the hydrophilic block play important roles to determine the assembled structures. In order to explore those interesting structures and properties, a variety of amphiphilic block polymers have been prepared [4–9,18]. The amphiphilic block copolymers have been prepared by the anionic living polymerization [4,8,15], atom transfer radical polymerization (ATRP) [19], and reversible addition–fragmentation chain transfer (RAFT) [20,21].

Azobenzene and its derivatives, which are well known for their reversible *trans–cis* photoisomerization, have been widely used as functional groups to prepare various photoresponsive polymers [22,23]. Recently, azobenzene-containing amphiphilic block copolymers have been prepared and tested for their self-assembling and photoresponsive properties [24–30]. A block

* Corresponding author. Tel.: +86 10 62784561; fax: +86 10 6279 6171.
E-mail address: wxg-dce@mail.tsinghua.edu.cn (X. Wang).

0032-3861/$ – see front matter © 2008 Elsevier Ltd. All rights reserved.
doi:10.1016/j.polymer.2008.11.010

copolymer composed of azobenzene-containing methacrylate and acrylic-acid blocks has been prepared. The polymer can form micellar aggregates in water and the aggregation can be reversibly altered upon UV and visible light illumination [24]. Also, a block copolymer with the azobenzene-containing block and 2-(dimethylamino)ethyl metharylate block has been prepared [27]. The polymer is water soluble and can self-assemble into polymeric micelles with core–shell structure. Block copolymer containing the hydrophobic block of side-on mesogenic units and hydrophilic PEG block has been reported [28]. The polymer can form vesicles under the influence of the solubility of the solvent. Azobenzene-containing block copolymers have also been synthesized by RAFT. The polymers show the ability to form vesicles with large size and light responsive property [29,30].

According to the spectroscopic features and isomerization behavior, azobenzene derivatives can be subdivided into three different types, i.e. azobenzene, aminoazobenzene and pseudo-stilbene [31]. The latter two-type azo compounds possess the overlapped n–π^* and π–π^* transition bands and their *cis*-form can quickly relax back to the *trans*-form. The polymers containing such chromophores possess interesting properties such as photoinduced anisotropy [22,23,32], surface-relief-grating (SRG) formation [33,34], and nonlinear optical (NLO) properties [35,36]. Recently, colloidal spheres containing pseudo-stilbene type azo chromophores have been prepared by using amphiphilic random copolymers [37], and polydispersed homopolymer [38,39]. The colloids can be stretched along the polarization direction of the laser beam upon the polarized light irradiation [38,39]. Because of the random nature of the amphiphilic polymers, the inner structure of the colloids is more difficult to be characterized compared with those formed from well-defined block polymers. Amphiphilic block copolymers bearing strong push–pull azo chromophores (pseudo-stilbene type) can be used to prepare the photodeformable colloids and other self-assembled structures. However, up till now, only few amphiphilic block copolymers containing such azo chromophores have been synthesized [40]. In a recent communication, we have reported the synthesis of an amphiphilic diblock copolymer that consists of hydrophilic PEG block and hydrophobic polymethacrylate block bearing side chain 4-amino-4′-cyanoazobenzene chromophores [41]. Photoinduced deformation was also observed for the spherical aggregates of the copolymer after the irradiation of a linearly polarized Ar^+ laser beam. However, up till now, a systematic study of block copolymers bearing strong push–pull type azo chromophores, concerning their synthesis, self-assembly in solution, and photo-responsive properties, is still lacking in the literature.

In the present work, a series of amphiphilic block copolymers bearing pseudo-stilbene type azo chromophores was synthesized. In the processes, precursor diblock copolymers (P(EMA$_m$-*b*-*t*BMA$_n$)) were synthesized by two-stage atom transfer radical polymerization (ATRP) of 2-(*N*-ethyl-*N*-phenylamino)ethyl methacrylate (EMA) and *tert*-butyl methacrylate (*t*BMA). The target block copolymers (P(CNAZO$_m$-*b*-MAA$_n$)) were obtained through the azo-coupling reaction to introduce the azo chromophores and the following hydrolysis to remove the *tert*-butyl groups. The block copolymers showed ability to form micellar aggregates in THF/H_2O solutions induced by the increase of the water content. The aggregate formation and photoresponsive behavior upon polarized Ar^+ laser irradiation were thoroughly investigated. The experimental details, results and discussions will be presented in the following sections.

2. Experimental section

2.1. Materials

2-(*N*-Ethyl-*N*-phenylamino)ethyl methacrylate (EMA) was synthesized by esterification reaction according to the procedure published previously [41]. Acetone was refluxed over $KMnO_4$ for 6 h and then distilled before use. Tetrahydrofuran (THF) was purified by distillation with sodium and benzophenone. *tert*-Butyl methacrylate (*t*BMA) (98%, TCI) was distilled and stored at 0 °C before use. CuCl (99%, Aldrich) was purified by stirring overnight in acetic acid. After filtration, the salt was washed orderly with a large amount of ethanol and ether. After that, the solid was dried in a vacuum oven for 24 h. Deionized water (resistivity > 18 MΩ cm) was obtained from a Milli-Q water purification system and used for the following experiments. The other solvents and reagents were purchased commercially and used without further purification.

Table 1
Molecular weights and polydispersity indexes of the polymer and copolymers.

Sample	M_n^{GPC}	M_w/M_n^{GPC}	M_n^{NMR}
PEMA	23 000	1.13	–
P(EMA$_{100}$-*b*-*t*BMA$_5$)	16 200	1.14	24 000
P(CNAZO$_{100}$-*b*-*t*BMA$_5$)	20 600	1.18	36 900
P(CNAZO$_{100}$-*b*-MAA$_5$)	18 200	1.28	36 600
P(EMA$_{100}$-*b*-*t*BMA$_{13}$)	17 200	1.14	25 100
P(CNAZO$_{100}$-*b*-*t*BMA$_{13}$)	20 800	1.18	38 000
P(CNAZO$_{100}$-*b*-MAA$_{13}$)	18 700	1.24	37 300
P(EMA$_{100}$-*b*-*t*BMA$_{23}$)	17 800	1.16	26 600
P(CNAZO$_{100}$-*b*-*t*BMA$_{23}$)	21 200	1.18	39 500
P(CNAZO$_{100}$-*b*-MAA$_{23}$)	19 600	1.25	38 200

2.2. Poly(2-(N-*ethyl*-N-*phenylamino*)*ethyl methacrylate*) (PEMA)

p-Toluenesulfonyl chloride (38.12 mg, 0.20 mmol) and CuCl (39.6 mg, 0.40 mmol) were added into a 25 mL Schlenk flask. After degassed and back-filled with argon three times, a mixture of acetone (4 mL), 2-(*N*-ethyl-*N*-phenylamino)ethyl methacrylate (EMA) (4.66 g, 20.0 mmol) and 1,1,4,7,10,10-hexamethyltriethylenetetramine (HMTETA) (108.8 μL, 0.40 mmol) was added into the flask. The solution was degassed again through three freeze–pump–thaw cycles. Then, the flask was immersed in an oil bath at 50 °C and the polymerization was carried out at the temperature for 16 h. The reaction was terminated by adding an excessive amount of THF. Then the mixture was passed through an alumina column to remove the catalyst. The filtrate was concentrated and poured into an excess amount of petrol ether. After the precipitate was collected and washed with petrol ether, the product was dissolved in THF and then precipitated again with petroleum ether. The final product was collected and then dried in a vacuum oven at 45 °C for 24 h. Yield: 76%. d*n*/d*c* = 0.154 mL/g. GPC: $M_n = 23\,000$, $M_w/M_n = 1.13$. ^{1}H NMR ($CDCl_3$), δ (ppm): 0.69–0.96 (m, CH_3, 3H), 1.12 (br, CH_3, 3H), 1.55–1.95 (m, CH_2, 2H), 3.33 (br, CH_2, 2H), 3.46 (br, CH_2, 2H), 4.01 (br, CH_2, 2H), 6.68 (br, Ar–H, 3H), 7.17 (br, Ar–H, 2H).

2.3. Poly(*EMA*$_m$-b-t*BMA*$_n$)

The block copolymers were obtained through ATRP of *tert*-butyl methacrylate (*t*BMA) by using poly(2-(*N*-ethyl-*N*-phenylamino)ethyl methacrylate) with chlorine terminal group as the macroinitiator. Three P(EMA$_m$-*b*-*t*BMA$_n$) samples with the same EMA block and three different lengths of the *t*BMA block were synthesized in this work. The molecular weights of the copolymers with different block lengths are summarized in Table 1. The synthesis of P(EMA$_{100}$-*b*-*t*BMA$_{13}$) is given here as a typical example.[1] Other copolymers were prepared through the similar procedure by adjusting the relative amount of *t*BMA. PEMA

[1] The figures in the subscript mean the number of the repeat units estimated from the molecular weight of PEMA and the ^{1}H NMR spectra of the copolymers.

(0.230 g, 0.01 mmol) and CuCl (9.9 mg, 0.10 mmol) were added into a 25 mL Schlenk flask. After degassed and back-filled with argon three times, a mixture of anisole (2 mL), *t*BMA (0.028 g, 0.2 mmol) and HMTETA (27.2 μL, 0.10 mmol) was added into the flask. The solution was degassed again through three freeze–pump–thaw cycles. Then, the flask was immersed in an oil bath at 80 °C and the polymerization was carried out at the temperature for 20 h. After the mixture was passed through an alumina column to remove the catalyst, the filtrate was concentrated and precipitated into a mixture of methanol and water (1/1, v/v). The precipitate was collected and then dried in a vacuum oven at 45 °C for 24 h. Yield: 0.188 g, 73%. GPC: $M_n = 17\,200$, $M_w/M_n = 1.14$. ^{1}H NMR ($CDCl_3$), δ (ppm): 0.69–0.96 (m, CH_3), 1.12 (br, CH_3, 3H), 1.42 (br, CH_3), 1.55–1.95 (m, CH_2), 3.33 (br, CH_2, 2H), 3.46 (br, CH_2, 2H), 4.01 (br, CH_2, 2H), 6.68 (br, Ar–H, 3H), 7.17 (br, Ar–H, 2H).

Other two P(EMA_m-*b*-*t*BMA_n) samples were prepared by using the similar conditions. The *t*BMA amounts used in the reactions were 0.014 g (0.1 mmol) for P(EMA_{100}-*b*-*t*BMA_5) and 0.042 g (0.3 mmol) for P(EMA_{100}-*b*-*t*BMA_{23}). The analytical results are given as follows: P(EMA_{100}-*b*-*t*BMA_5): GPC: $M_n = 16\,200$, $M_w/M_n = 1.14$. ^{1}H NMR ($CDCl_3$), δ (ppm): 0.70–1.00 (m, CH_3), 1.11 (br, CH_3, 3H), 1.42 (br, CH_3), 1.60–1.90 (m, CH_2), 3.34 (br, CH_2, 2H), 3.46 (br, CH_2, 2H), 4.01 (br, CH_2, 2H), 6.71 (br, Ar–H, 3H), 7.17 (br, Ar–H, 2H). P(EMA_{100}-*b*-*t*BMA_{23}): GPC: $M_n = 17\,800$, $M_w/M_n = 1.16$. ^{1}H NMR ($CDCl_3$), δ (ppm): 0.70–1.00 (m, CH_3), 1.11 (br, CH_3, 3H), 1.41 (br, CH_3), 1.60–1.95 (m, CH_2), 3.33 (br, CH_2, 2H), 3.46 (br, CH_2, 2H), 4.02 (br, CH_2, 2H), 6.70 (br, Ar–H, 3H), 7.17 (br, Ar–H, 2H).

2.4. P(*CNAZO*$_m$-b-t*BMA*$_n$)

The block copolymers were designed to contain 2-(*N*-ethyl-*N*-(4-(4′-cyanophenylazo) phenyl)amino)ethyl methacrylate (CNAZO) and *tert*-butyl methacrylate (*t*BMA) blocks. P($CNAZO_m$-*b*-*t*BMA_n) was synthesized by azo-coupling reaction of P(EMA_m-*b*-*t*BMA_n) with diazonium salt of 4-aminobenzonitrile. The synthesis of P($CNAZO_{100}$-*b*-*t*BMA_{13}) is given here as a typical example. The diazonium salt solution of 4-aminobenzonitrile was prepared by adding an aqueous solution of sodium nitrite (0.06 g, 0.87 mmol) dropwise into a solution of 4-aminobenzonitrile (0.089 g, 0.75 mmol) in a homogeneous mixture of sulfuric acid (0.15 mL) and glacial acetic acid (2.25 mL). The mixture was stirred at 0 °C for 5 min. The diazonium salt solution was added dropwise into the solution of P(EMA_{100}-*b*-*t*BMA_{13}) (0.126 g, 0.5 mmol in terms of the anilino group) in DMF (50 mL) at 0 °C. After the reaction was carried out at 0 °C for 12 h, the solution was poured into an excessive amount of water. The precipitate was collected by filtration and washed with water repeatedly. After drying the solid was dissolved with THF and then precipitated with petroleum ether. The precipitate was collected by filtration and dried in a vacuum oven at 40 °C for 24 h. Yield: 0.132 g, 69%. GPC: $M_n = 20\,800$, $M_w/M_n = 1.18$. ^{1}H NMR ($CDCl_3$), δ (ppm): 0.60–0.96 (m, CH_3), 1.12 (br, CH_3, 3H), 1.42 (br, CH_3), 1.55–1.95 (m, CH_2), 3.10–3.75 (m, CH_2, 4H), 4.04 (br, CH_2, 2H), 6.68 (br, Ar–H, 2H), 7.58 (br, Ar–H, 2H), 7.71 (br, Ar–H, 4H).

Other two P($CNAZO_m$-*b*-*t*BMA_n) samples were prepared by using the similar conditions. The amounts of 4-aminobenzonitrile used in the reactions were 0.089 g (0.75 mmol). The amounts of P(EMA_m-*b*-*t*BMA_n) used in the reactions were 0.12 g for P($CNAZO_{100}$-*b*-*t*BMA_5) and 0.133 g for P($CNAZO_{100}$-*b*-*t*BMA_{23}), which contain 0.5 mmol of the anilino groups in both cases. The analytical results are given as follows: P($CNAZO_{100}$-*b*-*t*BMA_5): GPC: $M_n = 20\,600$, $M_w/M_n = 1.18$. ^{1}H NMR ($CDCl_3$), δ (ppm): 0.60–0.95 (m, CH_3), 1.11 (br, CH_3, 3H), 1.42 (br, CH_3), 1.60–1.90 (m, CH_2), 3.10–3.75 (m, CH_2, 4H), 4.02 (br, CH_2, 2H), 6.70 (br, Ar–H, 2H), 7.56 (br, Ar–H, 2H), 7.70 (br, Ar–H, 4H). P($CNAZO_{100}$-*b*-*t*BMA_{23}): GPC: $M_n = 21\,200$, $M_w/M_n = 1.18$. ^{1}H NMR ($CDCl_3$), δ (ppm): 0.60–1.00 (m, CH_3), 1.11 (br, CH_3, 3H), 1.42 (br, CH_3), 1.60–1.90 (m, CH_2), 3.10–3.70 (m, CH_2, 4H), 4.02 (br, CH_2, 2H), 6.68 (br, Ar–H, 2H), 7.57 (br, Ar–H, 2H), 7.71 (br, Ar–H, 4H).

2.5. P(*CNAZO*$_m$-b-*MAA*$_n$)

P($CNAZO_m$-*b*-MAA_n) was prepared through a selective hydrolysis of P($CNAZO_m$-*b*-*t*BMA_n) to remove the *tert*-butyl groups from the *tert*-butyl methacrylate (*t*BMA) block. The preparation of P($CNAZO_{100}$-*b*-MAA_{13}) is given here as a typical example. Trifluoroacetic acid (1 mL) was slowly added into a dichloromethane solution of P($CNAZO_{100}$-*b*-*t*BMA_{13}) (100 mg in 20 mL) at 0 °C with vigorous stirring. The reaction was carried out at room temperature overnight. The solvent of the reaction mixture was removed by rotary evaporation. For purification, the copolymer obtained after the hydrolysis was dissolved in THF and precipitated with hexane for three times. Then the precipitate was collected by filtration and dried in a vacuum oven at 60 °C for 48 h. Yield: 0.065 g, 66%. GPC: $M_n = 18\,700$, $M_w/M_n = 1.24$. ^{1}H NMR (THF-d_8), δ (ppm): 0.60–0.95 (br, CH_3), 1.05 (br, CH_3, 3H), 1.65–1.95 (br, CH_2), 3.25–3.80 (m, CH_2, 4H), 4.05 (br, CH_2, 2H), 6.78 (br, Ar–H, 2H), 7.68 (br, Ar–H, 2H), 7.77 (br, Ar–H, 4H).

Other two P($CNAZO_m$-*b*-MAA_n) samples were prepared under the same conditions. The analytical results are given as follows: P($CNAZO_{100}$-*b*-MAA_5): GPC: $M_n = 18\,200$, $M_w/M_n = 1.28$. ^{1}H NMR (THF-d_8), δ (ppm): 0.65–0.90 (br, CH_3), 1.04 (br, CH_3, 3H), 1.65–1.95 (br, CH_2), 3.25–3.80 (m, CH_2, 4H), 4.05 (br, CH_2, 2H), 6.76 (br, Ar–H, 2H), 7.66 (br, Ar–H, 2H), 7.75 (br, Ar–H, 4H). P($CNAZO_{100}$-*b*-MAA_{23}): GPC: $M_n = 19\,600$, $M_w/M_n = 1.25$. ^{1}H NMR (THF-d_8), δ (ppm): 0.65–0.90 (br, CH_3), 1.03 (br, CH_3, 3H), 1.65–1.95 (br, CH_2), 3.25–3.80 (m, CH_2, 4H), 4.04 (br, CH_2, 2H), 6.76 (br, Ar–H, 2H), 7.67 (br, Ar–H, 2H), 7.76 (br, Ar–H, 4H).

2.6. Preparation of micellar aggregates

To prepare the micellar aggregates, P($CNAZO_m$-*b*-MAA_n) solutions were prepared by dissolving the copolymers in THF with an initial concentration of 0.1 mg/mL. A suitable amount of deionized water (50 wt%) was slowly added into the THF solutions via syringe pump at a preset rate. Then an excessive amount of deionized water was added into the suspensions to quench the micellar structures formed in process. The resulting suspensions were dialyzed against deionized water for 72 h to remove THF. The light scattering measurements were performed to determine the parameters such as the critical water content (CWC) and the hydrodynamic radius (R_h).

2.7. Photoinduced shape deformation study

The samples for photoinduced shape deformation study were prepared by dropping the suspensions of the micellar aggregates onto the copper grids coated with a thin polymer film and then dried in a 30 °C vacuum oven for 24 h. The laser irradiation experiments were performed at room temperature under an air ambient condition. A linearly polarized Ar^+ laser beam was used as the light source. The spatially filtered laser beam was expanded and collimated to obtain a beam with the intensity of 150 mW/cm^2. The laser beam was incident perpendicularly to the grid surfaces containing the aggregates. After irradiation for different time periods, the TEM observations were carried out to detect the shape deformation.

2.8. Characterization

^{1}H NMR spectra were recorded on a JEOL JNM-ECA300 spectrometer (300 MHz for proton) by using $CDCl_3$ as the solvent. In the

case of P(CNAZO$_m$-*b*-MAA$_n$), THF-d_8 was used as the solvent. The molecular weights and molecular weight distributions were determined by using a gel permeation chromatography (GPC) apparatus with THF as eluent (1 mL/min) at 25 °C. The instrument was equipped with a refractive index (RI) detector (Wyatt Optilab rEX) and fitted with a PLgel 5 μm mixed-D column. The molecular weights were determined from a calibration curve based on linear polystyrene standards. The molecular weight of PEMA was calculated from the response of a laser light scattering detector (Wyatt miniDAWN) that was connected to the GPC line with a laser source of 633 nm. The dn/dc value of PEMA was measured using the Wyatt Optilab rEX. UV–vis spectra were recorded by using an Agilent 8453 UV–vis spectrophotometer. Thermal stability and thermal phase transition temperatures of the polymers were tested by using TA Instruments TGA 2050 and DSC 2920 with a heating rate of 10 °C/min in nitrogen atmosphere. Laser light scattering experiments were performed on a commercial LS instrument (ALV/DLS/SLS-5022F) equipped with a multi-τ digital time correlator (ALV/LSE-5003) and a solid-state laser (Uniphase, output power = 22 mW, at $\lambda = 632.8$ mn). The morphologies of the micellar aggregates were examined using a JEOL JSM-1200EX transmission electron microscope (TEM) with the accelerating voltage of 120 kV.

3. Results and discussion

In this study, a series of amphiphilic block copolymers bearing pseudo-stilbene type azo chromophores (P(CNAZO$_m$-*b*-MAA$_n$)) was synthesized through the post-polymerization functionalization scheme. The reason to adopt this reaction scheme is mainly due to the low efficiency of the radical polymerization of the monomers, which is caused by the strong inhibition effect of the azo chromophores to the radical polymerization. For example, by using AIBN (10 wt%) as initiator, the polymerization of 4′-((2-(acryloyloxy)ethyl)ethylamino)-4-nitroazobenzene took about 4 days to obtain a polymer with the molecular weight of 4000 [42,43]. As the active radical concentration is even lower in ATRP, the polymerization of such monomers should be more difficult to be carried out. Moreover, the post-polymerization functionalization can have advantage to avoid possible side reactions of the radicals with the azo chromophores. It has been reported that such post-polymerization azo-coupling reaction can have a high conversion reaching about 100% [35,36]. In order to study the influence of the hydrophobic and hydrophilic block ratio on the properties, three P(CNAZO$_m$-*b*-PMAA$_n$) samples with the same CNAZO block length and three different MAA block lengths were prepared (Table 1). The aggregate formation was explored by using the copolymers and the photoresponsive properties of the micellar aggregates were investigated subsequently.

3.1. Block copolymer synthesis

The synthetic route of the amphiphilic block azo copolymers is given in Scheme 1. Firstly, poly(2-(*N*-ethyl-*N*-phenylamino)ethyl methacrylate) (PEMA) was prepared by ATRP. By using PEMA with chlorine terminal group as the macroinitiator, P(EMA$_m$-*b*-*t*BMA$_n$) was obtained through ATRP of *tert*-butyl methacrylate (*t*BMA). Then, P(CNAZO$_m$-*b*-*t*BMA$_n$) was prepared by the azo-coupling reaction between P(EMA$_m$-*b*-*t*BMA$_n$) and the diazonium salt of 4-aminobenzonitrile. Finally, P(CNAZO$_m$-*b*-MAA$_n$) was obtained after the selective cleavage of the *tert*-butyl ester groups of P(EMA$_m$-*b*-*t*BMA$_n$).

In the first-stage ATRP reaction, *p*-toluenesulfonyl chloride was used as the initiator and CuCl/HMTETA was used as the catalyst. The monomer, 2-(*N*-ethyl-*N*-phenylamino)ethyl methacrylate (EMA), polymerized in acetone at 50 °C to give a well-defined homopolymer with a narrow molecular weight distribution. PEMA obtained in this process has a number average molecular weight of 23 000 with the polydispersity index of 1.13, which was determined by using a GPC–LS combination method. Figs. 1 and 2a give the GPC curve and ^{1}H NMR spectrum of the polymer.

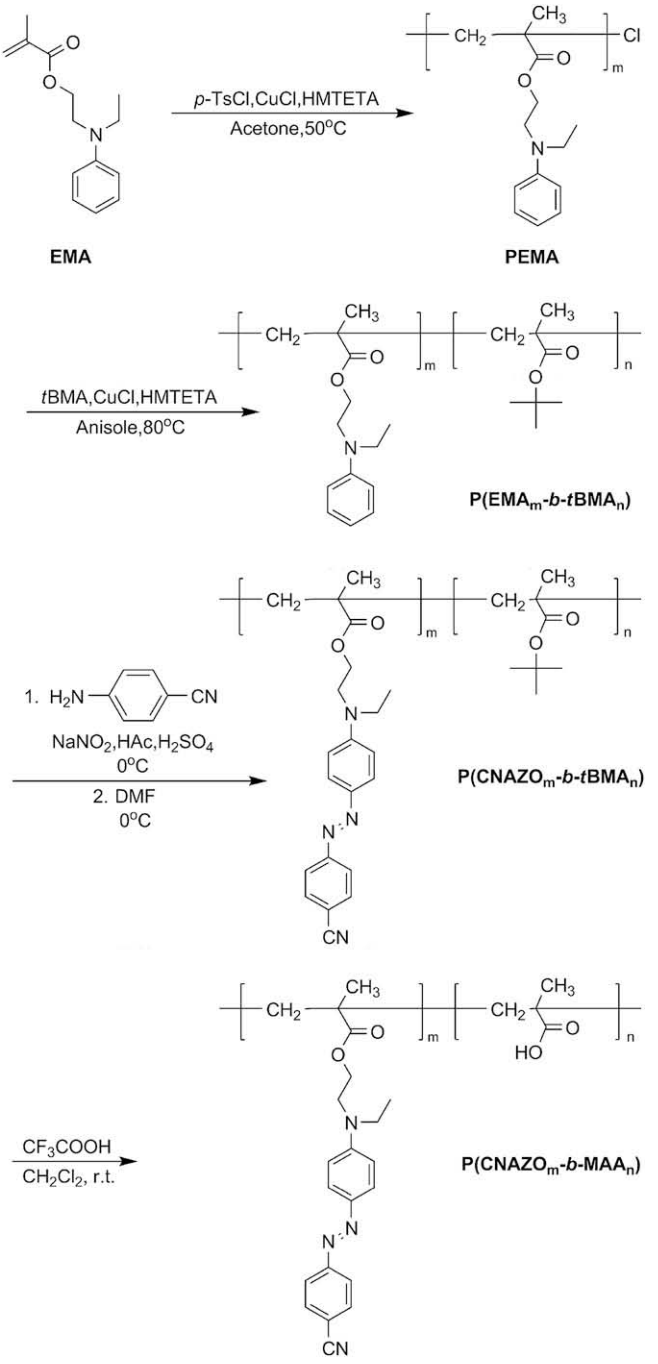

Scheme 1. Synthetic route of the amphiphilic block copolymers.

In the second-stage ATRP reaction, P(EMA$_m$-*b*-*t*BMA$_n$) was obtained by using the PEMA with chlorine terminal group as the macroinitiator. The polymerization was carried out at 80 °C by using anisole as the solvent in the presence of CuCl/HMTETA as the catalyst. Three copolymers with the same EMA block length ($m = 100$) and different *t*BMA block lengths ($n = 5$, 13, 23) were prepared by this method. The molecular weights and distributions of the copolymers are summarized in Table 1. The GPC characterization reveals the successful growth of *t*BMA blocks from the PEMA macroinitiator. Fig. 1 gives the GPC curves of

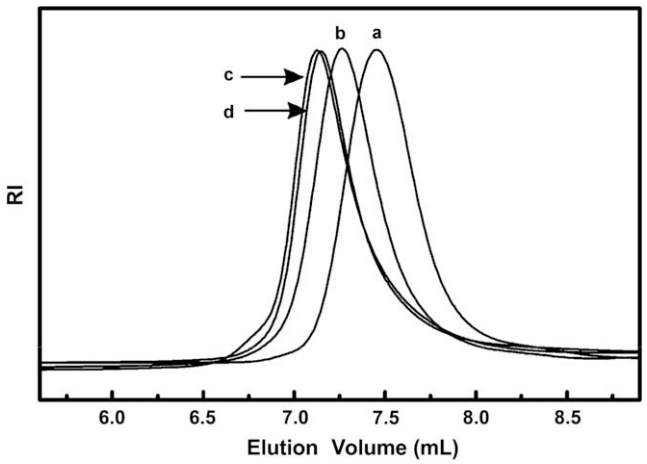

Fig. 1. GPC traces of a series of polymer and copolymers: a: PEMA, b: P(EMA$_{100}$-*b*-*t*BMA$_{23}$), c: P(CNAZO$_{100}$-*b*-*t*BMA$_{23}$), d: P(CNAZO$_{100}$-*b*-MAA$_{23}$).

P(EMA$_{100}$-*b*-*t*BMA$_{23}$) as a typical example. After introducing the *t*BMA block, the GPC trace shifts to the higher molecular weight region compared to the peak of PEMA. The number of the repeat

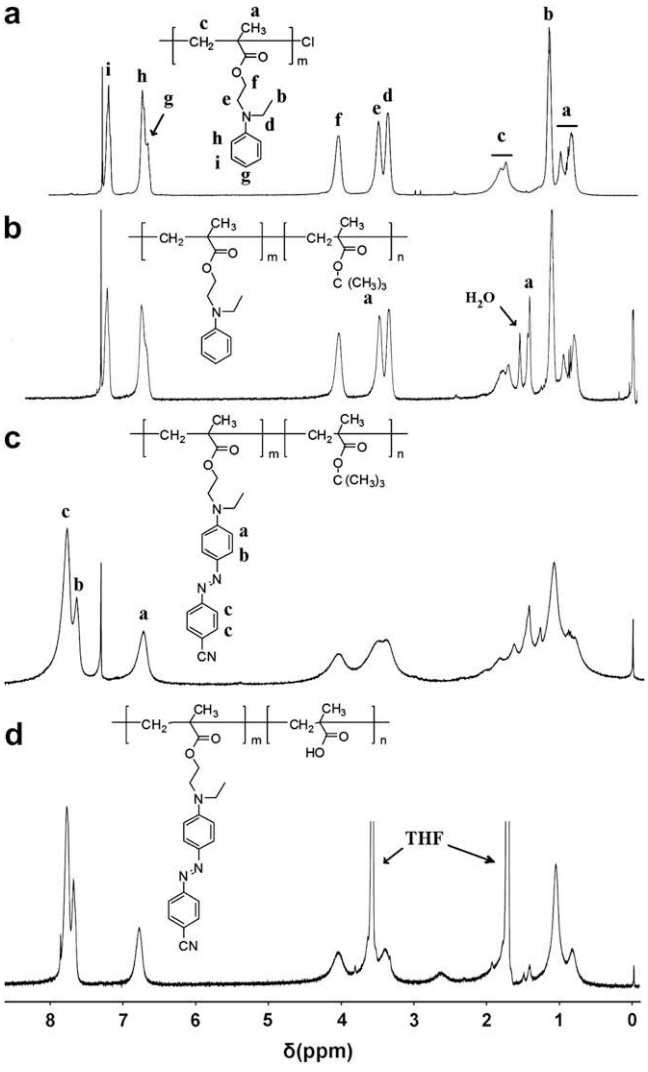

Fig. 2. ^{1}H NMR spectra of a series of polymer and copolymers: a: PEMA, b: P(EMA$_{100}$-*b*-*t*BMA$_{23}$), c: P(CNAZO$_{100}$-*b*-*t*BMA$_{23}$), d: P(CNAZO$_{100}$-*b*-MAA$_{23}$).

units of the *t*BMA blocks was calculated from the ^{1}H NMR spectra of the P(EMA$_m$-*b*-*t*BMA$_n$) (Fig. 2b) according to the equation:

$$n = (I_{1.42} \times 2 \times 100)/(I_{4.01} \times 9) \quad (1)$$

where 100 is the number of the repeat units of PEMA. The results indicate that the *t*BMA blocks with different lengths have been covalently bonded to the PEMA blocks (Table 1). The structure unit ratios of EMA to *t*BMA are 100:5, 100:13 and 100:23 for P(EMA$_{100}$-*b*-*t*BMA$_5$), P(EMA$_{100}$-*b*-*t*BMA$_{13}$), and P(EMA$_{100}$-*b*-*t*BMA$_{23}$), respectively.

The azo block copolymer (P(CNAZO$_m$-*b*-*t*BMA$_n$)) was obtained through the azo-coupling reaction between P(EMA$_m$-*b*-*t*BMA$_n$) and the diazonium salt of 4-aminobenzonitrile. The azo-coupling reaction between the precursor polymers and diazonium salt can be carried out in polar organic solvents [35,36]. In the present work, the post-polymerization azo-coupling reactions were performed by using DMF as the solvent. The characterization results reveal that nearly all the anilino moieties in the precursor polymers are converted to 4-amino-4′-cyanoazobenzene moieties. Fig. 2c shows the ^{1}H NMR spectrum of P(CNAZO$_{100}$-*b*-*t*BMA$_{23}$) as a typical example. Comparing to the spectrum of P(EMA$_{100}$-*b*-*t*BMA$_{23}$) (Fig. 2b), the 6.63 ppm resonance signal, corresponding to the protons in the *para*-positions of the anilino moieties in PEMA block, disappears completely after the azo-coupling reaction. Meanwhile, all the resonance signals of the protons in *meta*-positions of the amino groups shift from 7.17 ppm to lower magnetic field (7.58 ppm). The spectral variation is caused by the increase of the conjugated length and presence of the electron-withdrawing groups after the formation of the azobenzene moieties. These results indicate that the azo-coupling reactions occur at the *para*-positions of the anilino moieties of PEMA block and the conversion of the reaction is nearly 100%. The GPC curve of P(CNAZO$_{100}$-*b*-*t*BMA$_{23}$) is shown in Fig. 1 as a typical example. After azo-coupling reaction, the GPC trace shifts to higher molecular weight region. On the other hand, there is almost no change in the polydispersity index after the post-polymerization functionalization. The results are the same for the other two P(CNAZO$_m$-*b*-*t*BMA$_n$) copolymers.

The target amphiphilic block copolymers (P(CNAZO$_m$-*b*-MAA$_n$)) were prepared via the selective hydrolysis of P(CNAZO$_m$-*b*-*t*BMA$_n$). The hydrolysis was completed by using anhydrous trifluoroacetic acid as the hydrolyzing catalyst, which has been reported to be able to selectively split the *tert*-butyl ester linkage [44,45]. The most conclusive evidence for the success of the selective hydrolysis is provided by ^{1}H NMR spectroscopy. Fig. 2c and d shows the ^{1}H NMR spectra of P(CNAZO$_{100}$-*b*-*t*BMA$_{23}$) and P(CNAZO$_{100}$-*b*-MAA$_{23}$) in $CDCl_3$ and deuterated THF, which are good solvents for the copolymers. The resonance signal at 1.4 ppm in Fig. 2c, resulting from the *tert*-butyl protons of the *t*BMA block, is completely disappeared in (d). It indicates that the *tert*-butyl ester groups convert to carboxyl groups with a high yield. At the same time, there is almost no spectral change before and after hydrolysis for the resonances peaked at 0.6–0.9 and 1.1 ppm, which come from the methyl protons attached to the main-chain and the azobenzene-containing side chains. This observation reveals that the hydrolysis reaction occurs selectively and has no effect on the azobenzene-containing side chains. The GPC study shows that the molecular weights of the polymers decrease slightly after hydrolysis (Fig. 1 and Table 1).

3.2. Thermal properties and spectral feature

The phase transition temperatures of the polymers were examined by DSC in the N_2 ambience. To eliminate the effect of thermal history on the phase transitions, all the samples were heated to 150 °C, held at the temperature for 1 min and then

rapidly cooled down to −30 °C with liquid nitrogen. All DSC data reported here were obtained from the second-round scans after the quenching treatment. The DSC curves of a series of the polymer and copolymers are shown in Fig. 3. The curves reveal that all the polymer and copolymers show phase transition behavior of amorphous polymers. The glass transition temperature (T_g) is 40 °C for both PEMA and P(EMA$_{100}$-*b*-*t*BMA$_{23}$). The T_g increases to 130 °C after the post-polymerization azo-coupling reaction, which produces P(CNAZO$_{100}$-*b*-*t*BMA$_{23}$). The T_g of P(CNAZO$_{100}$-*b*-MAA$_{23}$) is also 130 °C although the hydrolysis has occurred on the *t*BMA units. For the block copolymers, there is only one T_g before thermal decomposition, which could be attributed to the low molar content of the *t*BMA and MAA blocks. In this case, the *t*BMA and MAA blocks could not aggregate to form a separate phase. The fact that PEMA and P(EMA$_m$-*b*-*t*BMA$_n$) show similar T_g could be attributed to the same reason. On the other hand, after the formation of the azo chromophores, T_g of the block copolymer is dramatically increased. Similar results have been reported for homopolymers after the post-polymerization azo-coupling reactions [35,36]. This result also indicates that the phase behavior of the copolymers is predominately determined by the CNAZO blocks.

The thermal decomposition of the polymer and copolymers was studied by TGA. The TGA curves of a series of the polymer and copolymers are given in Fig. 4. PEMA shows two principal weight losses starting at 220 and 330 °C (curve a). For P(EMA$_{100}$-*b*-*t*BMA$_{23}$), the first weight loss temperature increases to 250 °C, which corresponds to the introduction of the *t*BMA block (curve b). P(CNAZO$_{100}$-*b*-*t*BMA$_{23}$) shows three obvious decomposition weight losses starting at 250, 290 and 350 °C. After the hydrolysis of the *t*BMA units to yield P(CNAZO$_{100}$-*b*-MAA$_{23}$), the first weight loss temperature decreases from 250 to 210 °C. The TGA curves of the other two series of the block copolymers show similar decomposition behavior.

Fig. 5 shows the UV–vis spectra of P(CNAZO$_{100}$-*b*-*t*BMA$_{23}$) and P(CNAZO$_{100}$-*b*-MAA$_{23}$) in THF solutions (0.01 mg/mL). Both copolymers show typical spectral characteristics of the pseudo-stilbene type azo chromophores, in which only one strong absorption band appears in the visible wavelength range. The π–π* transition bands of both P(CNAZO$_m$-*b*-*t*BMA$_n$) and P(CNAZO$_m$-*b*-MAA$_n$) appear at 442 nm (λ_{max}). The hydrolysis of butyl ester groups does not show influence on the spectra of the copolymers.

3.3. Aggregate formation and morphologies

The micellar aggregates of P(CNAZO$_m$-*b*-MAA$_n$) were prepared by using a procedure developed by Eisenberg and Zhang [7,8]. In the process, homogeneous solutions were prepared by dissolving the amphiphilic azo block copolymers in anhydrous THF, which is a good solvent for both blocks. Deionized water, a selective solvent for MAA block, was gradually added into the polymer solutions. As the water content increased, the solubility of the mixed solvent continually became worse for the hydrophobic block, which triggered the aggregation of the dissolved polymer chains. Static light scattering (SLS) was used to monitor the aggregation process. Fig. 6 shows typical curves of scattered light intensity as a function of water content in the solvents. When the water content is low, the scattered light intensity is almost zero and remains unchanged, which indicates that the polymer chains are well dissolved in solutions. When the water content reaches a critical value, the scattered light intensity abruptly increases. This value has been defined as the critical water content (CWC), which means that the polymer chains start to aggregate at this critical point [12]. The CWC depends on both the initial concentration of polymer in the solution and the polymer composition. In the present study, the initial concentrations of the copolymer solutions were the same (0.1 mg/mL). For the three different P(CNAZO$_m$-*b*-MAA$_n$) samples, P(CNAZO$_{100}$-*b*-MAA$_5$) shows the CWC of 14% (wt%), and both P(CNAZO$_{100}$-*b*-MAA$_{13}$) and P(CNAZO$_{100}$-*b*-MAA$_{23}$) show the CWC of 18% (wt%). As the water contents further increase above CWC, the scattered light intensity keeps rapid increase and reaches a plateau when water contents

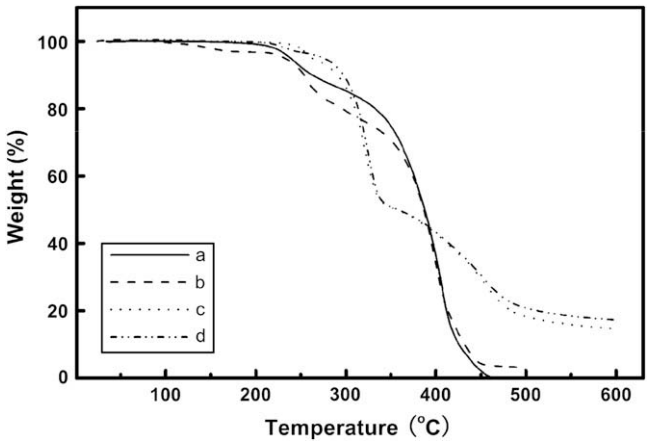

Fig. 4. TGA curves of a series of polymer and copolymers: a: PEMA, b: P(EMA$_{100}$-*b*-*t*BMA$_{23}$), c: P(CNAZO$_{100}$-*b*-*t*BMA$_{23}$), d: P(CNAZO$_{100}$-*b*-MAA$_{23}$).

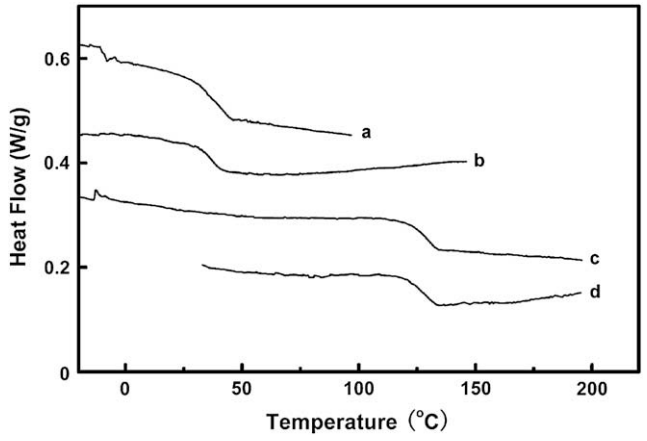

Fig. 3. DSC heating curves of a series of polymer and copolymers: a: PEMA, b: P(EMA$_{100}$-*b*-*t*BMA$_{23}$), c: P(CNAZO$_{100}$-*b*-*t*BMA$_{23}$), d: P(CNAZO$_{100}$-*b*-MAA$_{23}$).

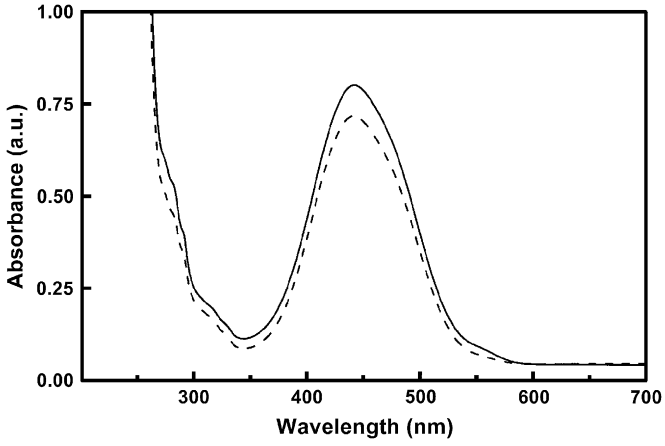

Fig. 5. UV–vis spectra of the THF solutions of P(CNAZO$_{100}$-*b*-MAA$_{23}$) (solid line) and P(CNAZO$_{100}$-*b*-*t*BMA$_{23}$) (dashed line).

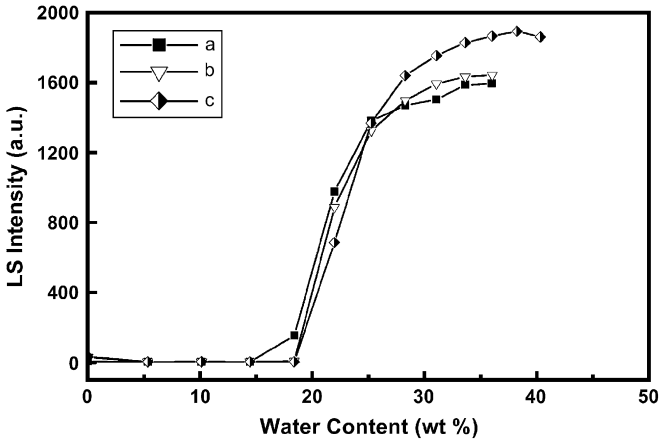

Fig. 6. Scattered light intensity as a function of the water content in H_2O/THF solutions of: a: P(CNAZO$_{100}$-*b*-MAA$_5$), b: P(CNAZO$_{100}$-*b*-MAA$_{13}$), c: P(CNAZO$_{100}$-*b*-MAA$_{23}$). The initial concentrations of the copolymers in THF were 0.1 mg/mL.

approach 35–45% (wt%). In this water content range, the polymer chain aggregation is almost completed. In order to prepare stable suspensions of the aggregates, deionized water was continually added until the water content reached 50% (wt%). Then an excessive amount of water was poured into the micelle suspensions to "quench" the structures formed in the process. After that, the suspensions were dialyzed against water to remove the THF.

The morphologies and sizes of the aggregates were studied by transmission electron microscopy (TEM) and dynamic light scattering (DLS). The morphologies of the aggregates observed by TEM show a sharp contrast without staining treatment. Fig. 7a gives a typical TEM image of P(CNAZO$_{100}$-*b*-MAA$_5$) aggregates. The aggregates were obtained under the conditions where the water-adding rate was 7.2 mL/h and the initial polymer concentration was 0.1 mg/mL. The TEM observation shows that P(CNAZO$_{100}$-*b*-PMAA$_5$) molecules form spherical aggregates with diameters most in range from 150 to 200 nm. Fig. 7b gives the size distribution of the aggregates estimated from the TEM observations. It indicates that the aggregates possess an average diameter of 175 nm. The aggregates obtained from other two amphiphilic block copolymers, P(CNAZO$_{100}$-*b*-PMAA$_{13}$) and P(CNAZO$_{100}$-*b*-PMAA$_{23}$), show similar spherical morphologies but different average sizes. The average sizes of the aggregates were characterized by the average hydrodynamic diameter (D_h) measured by dynamic light scattering (DLS). Fig. 8 shows the influences of the water-adding rate and the hydrophilic block length on the D_h of the copolymers. The results indicate that when the water-adding rate is lower than 7 mL/h, the average diameter rapidly decreases with the increase of the water-adding rate. When the water-adding rate is higher than 7 mL/h, the average diameter slightly decreases with the increase of the water-adding rate (Fig. 8a). Under the same water-adding rate (7.2 mL/h), the average diameter of the micellar aggregates decreases as the length of the hydrophilic block (MAA block) increases (Fig. 8b).

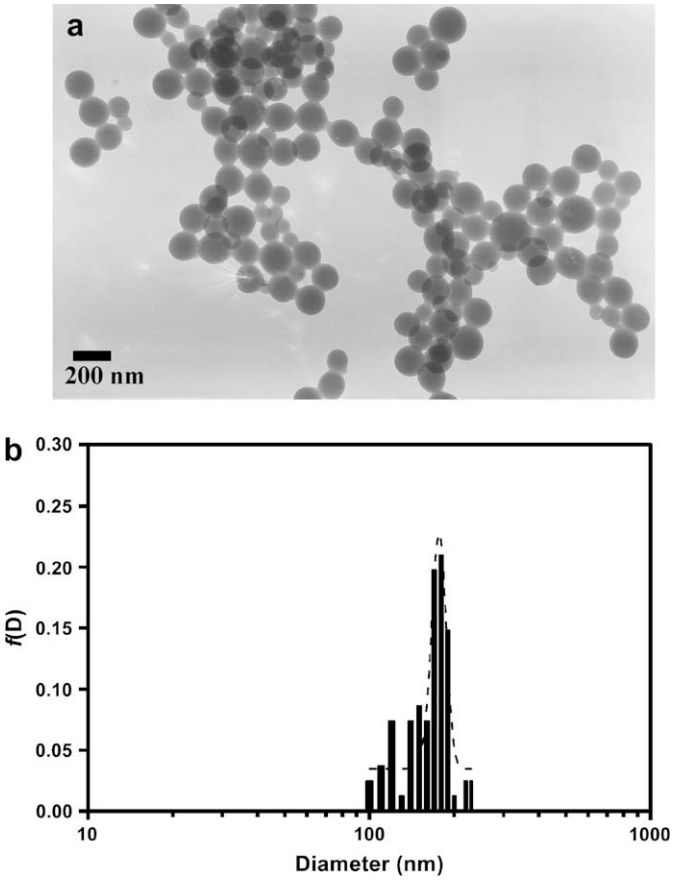

Fig. 7. (a) A typical TEM image of micellar aggregates of P(CNAZO$_{100}$-*b*-MAA$_5$). (b) Diameter distribution of the aggregates estimated from the TEM images, the dashed line represents the curve from Gaussian fitting. The initial concentration of the copolymer in THF was 0.1 mg/mL and the water-adding rate was 7.2 mL/h.

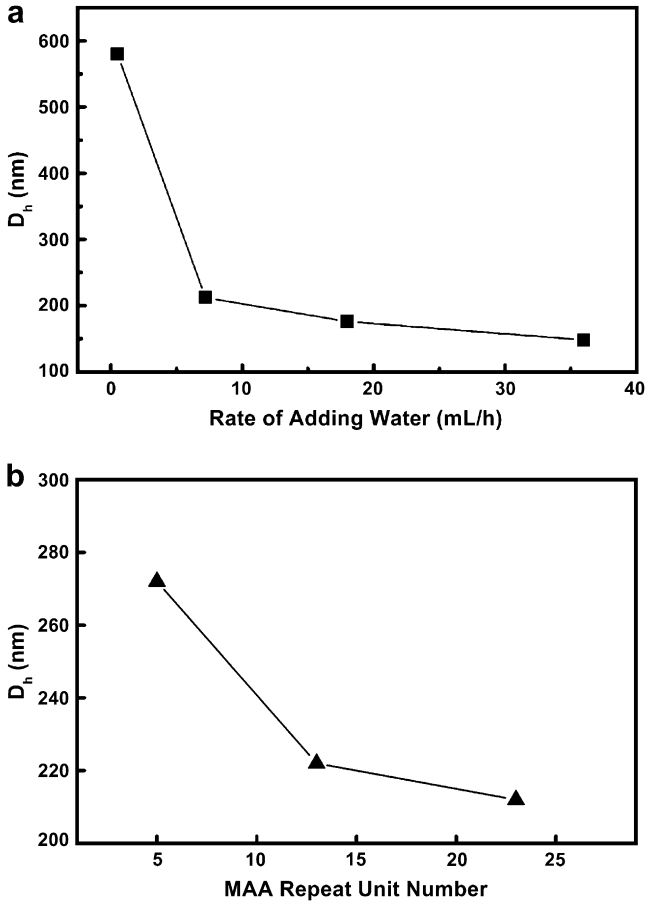

Fig. 8. Hydrodynamic diameters (D_hs) of the micellar aggregates (a) as a function of the water-adding rate for P(CNAZO$_{100}$-*b*-MAA$_{23}$), the initial polymer concentration in THF was 0.1 mg/mL; (b) as a function of the repeat unit number of MAA block, obtained by the same rate of water addition (7.2 mL/h).

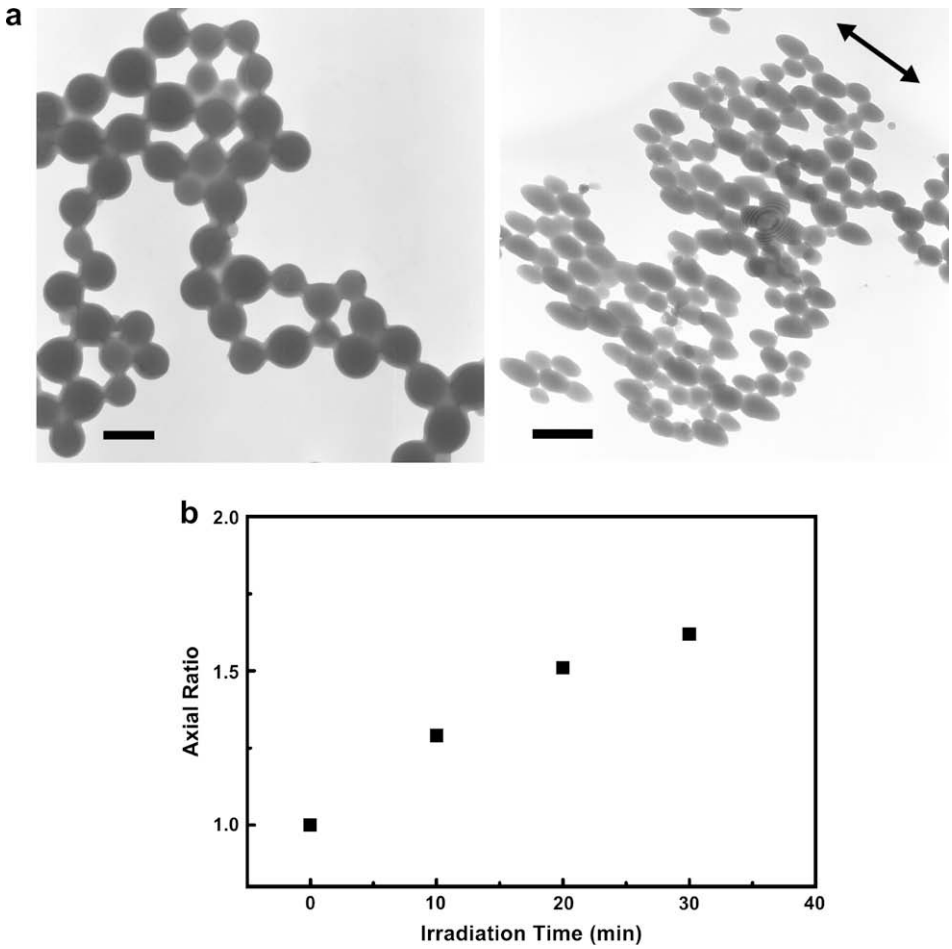

Fig. 9. (a) TEM images of micellar aggregates before and after the irradiation of Ar^+ laser beam for 30 min: (left) before irradiation, scale bar = 500 nm, (right) after irradiation, scale bar = 1000 nm. The initial concentration of P($CNAZO_{100}$-*b*-MAA_{23}) in THF was 0.1 mg/mL and the water-adding rate was 0.5 mL/h. The arrow represents the polarization direction of the laser beam. (b) Plot of the average axial ratio (l/d) vs the irradiation time.

According to the relative molecular weights of the hydrophobic and hydrophilic blocks, the micellar aggregates obtained in this work are considered to be the 'crew-cut' type [8,12,13]. From both the aggregate size and its control factors, it has reason to believe that the aggregates were formed through an irreversible phase-separation, which produced aggregates with "quenched" cores mainly composed of the CNAZO blocks. The MAA blocks were distributed in the corona to stabilize the aggregates in aqueous suspension. However, some MAA blocks could also be buried in the cores during the aggregation process. As the incomplete separation between both blocks occurred in micellar aggregates, the average aggregate sizes were obviously larger than those estimated from

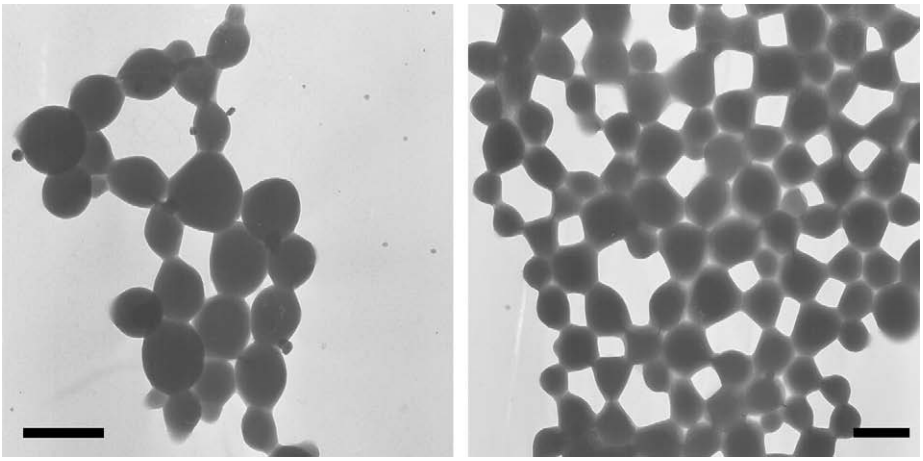

Fig. 10. Some typical TEM images of micellar aggregates of P($CNAZO_{100}$-*b*-MAA_{23}). The aggregates were irradiated with the Ar^+ laser beam for 30 min to induce the shape deformation and then treated by annealing at 150 °C for 24 h. Scale bar = 500 nm.

the block lengths. The increase in the MAA block length could increase the hydrophilic proportion in the corona, which reduced the surface tension and resulted in the decrease of the aggregate size.

3.4. Photoinduced shape deformation and recovery

The photoinduced shape deformation behavior of the micellar aggregates was investigated by using a linearly polarized Ar^+ laser beam as the light source. The aggregates with the average diameter of about 430 nm prepared from P(CNAZO$_{100}$-*b*-MAA$_{23}$) were used for the study. The samples were obtained by dropping the suspension on TEM copper grids. After drying, the aggregates were exposed to the linearly polarized Ar^+ laser beam (488 nm, 150 mW/cm^2) incident perpendicularly to the grid surfaces. After different irradiation time periods, the samples were observed by TEM. Fig. 9a shows typical TEM images of the aggregates before and after irradiation with the laser beam. The arrow on the right figure indicates the polarization direction of the laser beam. It can be seen that the spherical aggregates are elongated to form some ellipsoidal particles. The elongated direction of the aggregates is parallel to the polarization direction of the laser beam. The average axial ratios (l/d) of the aggregates, which were obtained by measuring statistically from 50 particles in the TEM images, are used to indicate the deformation degree. Fig. 9b shows the relationship between the average axial ratio and irradiation time. The result reveals that the average axial ratio increases almost linearly as the irradiation time increases in the testing period. After exposure to the laser beam for 30 min, the average axial ratio of the aggregates can reach 1.6. With the same light intensity and irradiation time, the deformation degree is similar to the aggregates formed from an amphiphilic diblock copolymer reported in our previous paper, which is composed of the same hydrophobic azobenzene-containing block and hydrophilic PEG block [41].

It is interesting to find that the deformed aggregates of the copolymers (such as P(CNAZO$_{100}$-*b*-MAA$_{23}$)) can be restored to the spherical shape by heat treatment. The shape recovery was tested by placing the copper grids with the aggregates in a vacuum oven at 150 °C for 24 h. The temperature is obviously higher than the T_g of P(CNAZO$_{100}$-*b*-MAA$_{23}$). After thermal annealing, the morphology of the aggregates was observed by TEM. Fig. 10 shows some typical TEM images of aggregates after the heat treatment. It can be clearly observed that the aggregates are restored to some less-regular spheres even though some aggregates are adhered with each other in the densely located zone. Although it has been well documented that the photoinduced surface-relief-gratings can be removed upon the thermal treatment, no shape recovery has been reported for the colloids formed from homopolymers, random copolymers and block copolymer [38,39,41,46,47]. More studies will be required to reveal the mechanism of the shape recovery and its correlation with polymer structure.

4. Conclusions

A new kind of amphiphilic block copolymers containing strong push–pull type azo chromophores has been developed in this work. P(CNAZO$_m$-*b*-MAA$_n$), composed of a hydrophobic block bearing 4-amino-4′-cyanoazobenzene moieties and a hydrophilic block of methacrylic acid units, was synthesized through four reaction steps. In the process, 2-(*N*-ethyl-*N*-phenylamino)ethyl methacrylate (EMA) and *tert*-butyl methacrylate (*t*BMA) were prepared through two-stage ATRP to form the precursor copolymers P(EMA$_m$-*b*-*t*BMA$_n$). Then, 4-amino-4′-cyanoazobenzene moieties were introduced through azo-coupling reaction of P(EMA$_m$-*b*-*t*BMA$_n$) with diazonium salt of 4-aminobenzonitrile. Finally, P(CNAZO$_m$-*b*-MAA$_n$) was obtained through selective hydrolysis of the *tert*-butyl ester linkages in the *t*BMA blocks. By this method, three P(CNAZO$_m$-*b*-MAA$_n$) copolymers with the CNAZO/MAA ratios of 100:5, 100:13, and 100:23 were synthesized. The amphiphilic block copolymers can form micellar spheres by gradually increasing the water content in the THF/H_2O mixed solvents. The sizes of the micellar aggregates depend on the hydrophilic block length and the water-adding rate. By irradiation with a linearly polarized Ar^+ laser beam, the spherical aggregates are elongated in the polarization direction. The deformation degree increases as the irradiation time increases in the testing period. The deformed aggregates can recover the original spherical shape after thermal annealing at a temperature above T_g of the block copolymers.

Acknowledgement

Financial support from the NSFC under projects 50533040 and 20774055 is gratefully acknowledged.

References

[1] Forster S. Top Curr Chem 2003;226:1–28.
[2] Liu SY, Armes SP. Curr Opin Colloid Interface 2001;6:249–56.
[3] Liu TB, Burger C, Chu B. Prog Polym Sci 2003;28:5–26.
[4] Wilhelm M, Zhao CL, Wang YC, Xu RL, Winnik MA, Mura JL, et al. Macromolecules 1991;24:1033–40.
[5] Balsara NP, Tirrell M, Lodge TP. Macromolecules 1991;24:1975–86.
[6] Kabanov AV, Nazarova IR, Astafieva IV, Batrakova EV, Alakhov VY, Yaroslavov AA, et al. Macromolecules 1995;28:2303–14.
[7] Zhang LF, Eisenberg A. Science 1995;268:1728–31.
[8] Zhang LF, Eisenberg A. J Am Chem Soc 1996;118:3168–81.
[9] Zhang LF, Yu K, Eisenberg A. Science 1996;272:1777–9.
[10] Bug ALR, Cates ME, Safran SA, Witten TA. J Chem Phys 1987;87:1824–33.
[11] Halperin A. Macromolecules 1987;20:2943–6.
[12] Zhang LF, Shen HW, Eisenberg A. Macromolecules 1997;30:1001–11.
[13] Shen HW, Zhang LF, Eisenberg A. J Phys Chem B 1997;101:4697–708.
[14] Linse P. Macromolecules 1994;27:6404–17.
[15] Noro A, Iinuma M, Suzuki J, Takano A, Matsushita Y. Macromolecules 2004; 37:3804–8.
[16] Terreau O, Luo LB, Eisenberg A. Langmuir 2003;19:5601–7.
[17] Terreau O, Bartels C, Eisenberg A. Langmuir 2004;20:637–45.
[18] See for example:
(a) Sommerdijk NAJM, Holder SJ, Hiorns RC, Jones RG, Nolte RJM. Macromolecules 2000;33:8289–94;
(b) Chang YC, Lee SC, Kim KT, Kim C, Reeves SD, Allcock HR. Macromolecules 2001;34:269–74;
(c) Liu SY, Billingham NC, Armes SP. Angew Chem Int Ed 2001;40:2328–31.
[19] Matyjaszewski K, Xia JH. Chem Rev 2001;101:2921–90.
[20] Chiefari J, Chong YK, Ercole F, Krstina J, Jeffery J, Le TPT, et al. Macromolecules 1998;31:5559–62.
[21] Chong YK, Le TPT, Moad G, Rizzardo E, Thang SH. Macromolecules 1999;32:2071–4.
[22] Delaire JA, Nakatani K. Chem Rev 2000;100:1817–45.
[23] Natansohn A, Rochon P. Chem Rev 2002;102:4139–75.
[24] Wang G, Tong X, Zhao Y. Macromolecules 2004;37:8911–7.
[25] Yu HF, Shishido A, Ikeda T, Iyoda T. Macromol Rapid Commun 2005; 26:1594–8.
[26] Yu HF, Okano K, Shishido A, Ikeda T, Kamata K, Komura M, et al. Adv Mater 2005;17:2184–8.
[27] Sin SL, Gan LH, Hu X, Tam KC, Gan YY. Macromolecules 2005;38:3943–8.
[28] Yang J, Pinol R, Gubellini F, Levy D, Albouy PA, Keller P, et al. Langmuir 2006;22:7907–11.
[29] Su W, Han K, Luo YH, Wang Z, Li YM, Zhang QJ. Macromol Chem Phys 2007;208:955–63.
[30] Su W, Luo YH, Yan Q, Wu S, Han K, Zhang QJ, et al. Macromol Rapid Commun 2007;28:1251–6.
[31] Rau H. In: Rabek JF, editor. Photochemistry and photophysics, vol. 2. Boca Raton: CRC Press; 1990. p. 119–41.
[32] Todorov T, Nikolova L, Tomava N. Appl Opt 1984:4309–12.
[33] Kim DY, Tripathy SK, Li L, Kumar J. Appl Phys Lett 1995;66:1166–8.
[34] Rochon P, Batalla E, Natansohn A. Appl Phys Lett 1995;66:136–8.
[35] Wang XG, Chen JI, Marturunkakul S, Li L, Kumar J, Tripathy SK. Chem Mater 1997;9:45–50.
[36] Wang XG, Kumar J, Tripathy SK, Li L, Chen JI, Marturunkakul S. Macromolecules 1997;30:219–25.
[37] Li YB, Deng YH, He YN, Tong XL, Wang XG. Langmuir 2005;21:6567–71.
[38] Li YB, He YN, Tong XL, Wang XG. J Am Chem Soc 2005;127:2402–3.

[39] Li YB, He YN, Tong XL, Wang XG. Langmuir 2006;22:2288–91.
[40] Hayakawa T, Horiuchi S, Shimizu H, Kawazoe T, Ohtsu M. J Polym Sci Part A Polym Chem 2002;40:2406–14.
[41] Wang DR, Ye G, Wang XG. Macromol Rapid Commun 2007;28:2237–43.
[42] Natansohn A, Rochon P, Gosselin J, Xie S. Macromolecules 1992;25: 2268–73.
[43] Ding LM, Russell TP. Macromolecules 2007;40:2267–70.
[44] Ma QG, Wooley KL. J Polym Sci Part A Polym Chem 2000;38: 4805–20.
[45] Ramakrishnan A, Dhamodharan R. Macromolecules 2003;36:1039–46.
[46] Lambeth RH, Moore JS. Macromolecules 2007;40:1838–42.
[47] Deng YH, Li N, He YN, Wang XG. Macromolecules 2007;40:6669–78.